Highly Transparent Films from Carboxymethylated Microfibrillated Cellulose: The Effect of Multiple Homogenization Steps on Key Properties

I. Siró,[1] D. Plackett,[1] M. Hedenqvist,[2] M. Ankerfors,[3] T. Lindström[3]

[1]*Risø National Laboratory for Sustainable Energy, Technical University of Denmark, P.O. Box 49, 4000 Roskilde, Denmark*
[2]*School of Chemical Science and Engineering, Fibre and Polymer Technology, Royal Institute of Technology—Kungliga Tekniska Högskolan, Teknikringen 56-58, SE-100 44 Stockholm, Sweden*
[3]*Innventia AB, P.O. Box 5604, SE-114 86 Stockholm, Sweden*

Received 15 March 2010; accepted 23 May 2010
DOI 10.1002/app.32831
Published online 9 September 2010 in Wiley Online Library (wileyonlinelibrary.com).

ABSTRACT: We produced microfibrillated cellulose by passing carboxymethylated sulfite-softwood-dissolving pulp with a relatively low hemicellulose content (4.5%) through a high-shear homogenizer. The resulting gel was subjected to as many as three additional homogenization steps and then used to prepare solvent-cast films. The optical, mechanical, and oxygen-barrier properties of these films were determined. A reduction in the quantity and appearance of large fiber fragments and fiber aggregates in the films as a function of increasing homogenization was illustrated with optical microscopy, atomic force microscopy, and scanning electron microscopy. Film opacity decreased with increasing homogenization, and the use of three additional homogenization steps after initial gel production resulted in highly transparent films. The oxygen permeability of the films was not significantly influenced by the degree of homogenization, whereas the mean tensile strength, modulus of elasticity, and strain at break were increased by two or three extra homogenization steps. © 2010 Wiley Periodicals, Inc. J Appl Polym Sci 119: 2652–2660, 2011

Key words: barrier; biopolymers; fibers; gas permeation; mechanical properties

INTRODUCTION

The conversion of cellulosic fibers into nanofibrils and their application in nanocomposites has attracted interest because of their high strength and stiffness combined with low weight, biodegradability, and renewability. The production of nanocellulose presents the opportunity to use the full potential of cellulose as a reinforcing material, which is considerable, given that the Young's modulus of the cellulose crystal is reported to be 220 GPa,[1] whereas tensile strength is estimated to be about 2 GPa.[2] Furthermore, as derived from the nanoscale dimensions, such material is expected to be free of light scattering (i.e., high light transmittance) when incorporated into films, which may be useful in, for example, the electronic device industry.[3,4] The extraction of nanofibrils from wood by mechanical means dates back to the early 1980s, when Herrick et al.[5] and Turbak et al.[6] succeeded in fibrillating wood pulp using a cyclic mechanical treatment with a high-pressure homogenizer to produce microfibrillated cellulose (MFC). Through this homogenization process, wood pulp was disintegrated and produced a material in which the fibers were moderately degraded and opened into their substructural microfibrils.[7] In principle, cellulose fibers can be disintegrated into 3–5 nm thick elementary microfibrils but because of the complicated multilayered structure of plant fibers and the interfibrillar hydrogen bonds, MFC generally consists of elementary fibril bundles of around 20 nm in width and several micrometers in length.[8] MFC is also sometimes referred to as *nanofibrillar* or *nanofibrillated cellulose.*[9–12]

A major obstacle to the successful commercialization of MFC has been the high energy consumption associated with the mechanical disintegration of the fibers into nanofibers, which often involves several passes through the disintegration device. Values around 20,000–30,000 kWh/ton are not uncommon, but higher values reaching 70,000 kWh/ton have also been reported.[13] However, through the combination of mechanical treatment with certain pretreatments (e.g., chemical- or enzyme-based), it is possible to significantly decrease the energy consumption.[14] Overall, a variety of mechanical treatments with high-pressure

Correspondence to: I. Siró (isir@risoe.dtu.dk).
Contract grant sponsors: European Union Sixth Framework Programme SUSTAINPACK project.

homogenization, grinding, cryocrushing, and combinations of such methods with chemical and enzymatic pretreatments have been investigated for the production of uniform cellulose nanofibrils. These methods were summarized elsewhere.[15] As an example of a chemical treatment, the introduction of carboxylate ions via the partial carboxymethylation of cellulose pulp results in electrostatic repulsion between the nanofibrils.[16] This charging makes the nanofibrils easier to liberate and also limits the aggregation of these nanofibrils.[12,17–19] Another approach to introducing charges onto cellulose fiber surfaces is the 2,2,6,6-tetramethylpiperidinyl-1-oxyl (TEMPO)-mediated oxidation of cellulose pulp, which has been described in detail elsewhere.[20–22]

The choice of raw material (i.e., the type of wood pulp) can also, to some extent, affect the energy required for conversion to MFC and the tendency of nanofibrils to form aggregates. As an example, the effect of hemicelluloses in facilitating nanofibrillation is recognized to be of some importance,[6] and this has been confirmed in more recent work.[23] High-hemicellulose-content pulps (e.g., sulfite pulp) should, therefore, be favorable for the preparation of MFC. Furthermore, evidence has indicated a tendency for aggregation during the Kraft processing of wood pulp when noncellulosic components (i.e., lignin and hemicelluloses) are removed; however, it is still not well understood how fibril aggregation affects the macroscale properties (e.g., strength) of pulp fiber.[24,25]

In our earlier research, two generations of MFC, differing in terms of the starting material and pretreatment, were investigated with respect to their structural and visual characteristics.[26] MFC generation 1 (MFC 1) was manufactured from a commercial bleached-sulfite-softwood pulp containing a relatively high amount of hemicellulose (13.8%), and MFC generation 2 (MFC 2) was produced from a commercial sulfite-softwood-dissolving pulp with a low hemicellulose content (4.5%). An enzymatic pretreatment and carboxymethylation was applied to ease the fibrillation process for MFC 1 and MFC 2, respectively. The study revealed a generally finer and more homogeneous size distribution of nanofibrils in films cast from MFC 2 relative to MFC 1. However, it also revealed the presence of some large-fiber cell-wall fragments in the MFC 2 films; this suggested incomplete disintegration of cellulose fibers. These larger fibril aggregate structures can compromise the transparency and the mechanical properties of MFC films. The aim of the research described here was to eliminate these large fiber aggregates in MFC 2 gels by means of additional homogenization steps and to determine how this further processing influenced the optical, mechanical, and oxygen-barrier properties of the cast films.

For the sake of clarity and to avoid ambiguity, some terminological notes are made. In the literature, the term *nanofibril aggregates* has been used by some authors as a synonym for MFC. In this article, the terms *large fiber fragments* and *fiber aggregates* are used to describe nonfibrillated and aggregated MFC nanofibers of several micrometers in diameter.

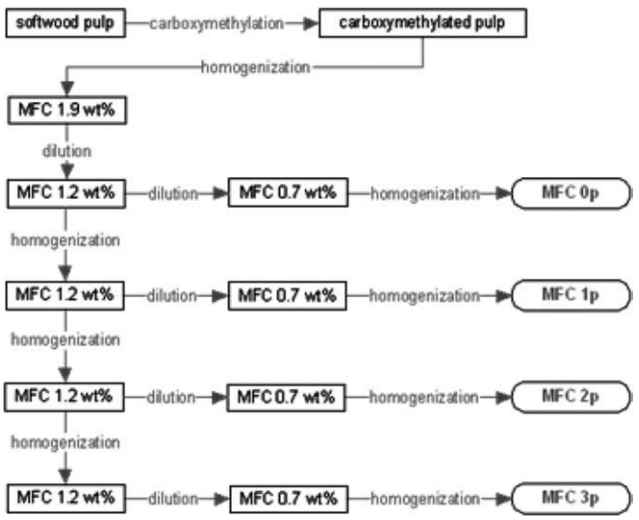

Figure 1 Scheme describing the procedure for MFC gel production.

EXPERIMENTAL

MFC preparation

MFC 2 was manufactured from a commercial sulfite-softwood-dissolving pulp (Domsjö Dissolving Plus, Domsjö Fabriker AB, Örnsköldsvik, Sweden) with a hemicellulose content of 4.5% and a lignin content of 0.6% at Innventia AB (previously STFI-Packforsk, Stockholm, Sweden). These composition data were obtained from the pulp supplier. Sulfite-dissolving pulp was chosen because, compared to Kraft pulp, it is easier to fibrillate and also contains a relatively high amount of cellulose relative to sulfite paper pulp. The pulp was first pretreated with a carboxymethylation procedure described in detail by Wågberg et al.,[16] and this was followed by high-pressure homogenization. The charge density of the carboxymethylated MFC was measured to be 586 μequiv/g with conductometric titration. Homogenization was performed in several steps, as illustrated in Figure 1. In the first step, a carboxymethylated pulp slurry (1.9 wt %) was passed once through the homogenizer. The resulting aqueous MFC gel was then diluted to 1.2 wt % and was homogenized a further one, two, or three times at this concentration. Finally, the samples were diluted to 0.7 wt % and were redispersed with one final pass through the homogenizer. The samples were denoted as 0p, 1p, 2p, and 3p on the basis of the number of extra homogenization steps to which the 1.2 wt % suspension was subjected. Thus, 0p, 1p, 2p, and 3p samples were

subjected to two, three, four, and five homogenization steps, respectively, in total.

Film casting

To cast films, the about 0.7 wt % MFC gels supplied by Innventia were further diluted to a concentration of about 0.35 wt % with deionized water. The suspensions were stirred by a magnetic stirrer for about 8 h under ambient conditions. Approximately 80 g of MFC aqueous suspension was then poured into a 120 × 120 mm^2 polystyrene Petri dish (Sigma-Aldrich, Copenhagen, Denmark), and the water was allowed to evaporate. We prepared films by drying the cast gels in an incubator (Climacell 111, MMM Medcenter Einrichtungen GmbH, Munich, Germany) under a controlled humidity at 50% relative humidity (RH) and 45°C for 48 h. The mean thickness of the resulting films was in the range 10.8–18 μm, as measured with a Mitutoyo micrometer (Mitutoyo Scandinavia AB, Upplands Väsby, Sweden) at 10 different spots.

Optical characteristics

MFC suspensions and films were examined with a Zeiss MC 80DX optical microscope (Carl Zeiss MicroImaging GmbH, Göttingen, Germany). The light transmittance of the films was measured over the 200–800-nm wavelength range with a Shimadzu 1700 UV–visible spectrophotometer (Shimadzu Europe GmbH, Duisburg, Germany). Film opacity, normalized to a film thickness of 25 μm and expressed as Absorbance × Nanometers, was calculated with an integration procedure described by Gontard et al.[27] Opacity was determined for three replicate films of each type. The visible spectra of the diluted MFC gels were recorded, and the gel opacity was also calculated.

Atomic force microscopy (AFM)

The surface topography of the MFC films was examined with a PSIA XE150 atomic force microscope (Park Systems, Suwon, South Korea). Standard silicon cantilevers with a theoretical spring constant of 40 N/m with an approximate resonance frequency of 300 kHz and a silicon tip of typical radius 10 nm were used (BS-Tap300Al, BudgetSensors, Innovative Solutions Bulgaria, Ltd., Sofia, Bulgaria). Film squares (20 × 20 μm^2) were scanned in tapping mode at a scan rate of 0.5 Hz. All AFM images were collected in air under ambient conditions. Images were processed with Gwyddion (Czech Metrology Institute, Brno, Czezh Republic), a modular freeware program for scanning probe microscopy data visualization and analysis.

Scanning electron microscopy (SEM)

The cross sections of the films were examined microscopically by means of an FEI Inspect S SEM (FEI Europe, Eindhoven, The Netherlands) equipped with a tungsten filament electron source with an acceleration voltage of 2 kV and a working distance of 8.6 mm. Film samples were embedded in epoxy resin and were coated with a thin layer of carbon (20 nm) before imaging.

Estimation of the fiber structure dimensions

The dimensions of the different fiber structures (i.e., nanofibrils and larger fiber aggregates) were estimated for all three microscopic techniques with the public domain Image J 1.41 image processing and analyzing software (National Institutes of Health, Bethesda, MD, USA).

X-ray diffractometry

X-ray diffraction was used to assess cellulose crystallinity within the MFC films. A Siemens D5000 X-ray diffractometer (Siemens Analytical and X-Ray Instruments Inc., Madison, WI, USA) equipped with a Co ($\lambda = 0.179$ nm) tube and a diffracted beam monochromator was used. Diffractograms were collected in a 2θ range of 3–30° at a rate of 1°/min with a resolution of 0.05°. The crystallinity index (C_i) was estimated from the diffraction patterns according to the Segal method with the following equation[28]:

$$C_i(\%) = \frac{I_{200} - I_{AM}}{I_{200}} \times 100 \quad (1)$$

where I_{200} and I_{AM} correspond to the intensities of the crystalline diffraction peak 200 (typically, at $2\theta \approx 26°$) and the minimum between the 200 and 110 peaks (I_{AM} at $2\theta \approx 22°$), respectively. This method assumes that the amorphous part of the cellulose shows equal intensity at both 2θ angles (22 and 26°).

Tensile tests

Tensile tests were performed according to ASTM D 882 on an Instron testing instrument (model 5566) (Instron, High Wycombe, UK) at 23°C and 50% RH. A load cell of 100 N was used, and the crosshead speed was 10 mm/min. The film thickness for each specimen was measured under these conditions with a Mitutoyo 10C-1125 μm and was recorded as the average of four measurements. Specimens were rectangular and 4 mm in width. The initial length between the clamps was 20 mm. The strain was defined as the clamp elongation relative to the initial length, and the modulus was obtained as the slope in a linear or near-linear part of the initial portion of the stress–strain curves, selected so as to exclude any initial nonlinear scatter. When fracture occurred at the clamps, the results were neglected.

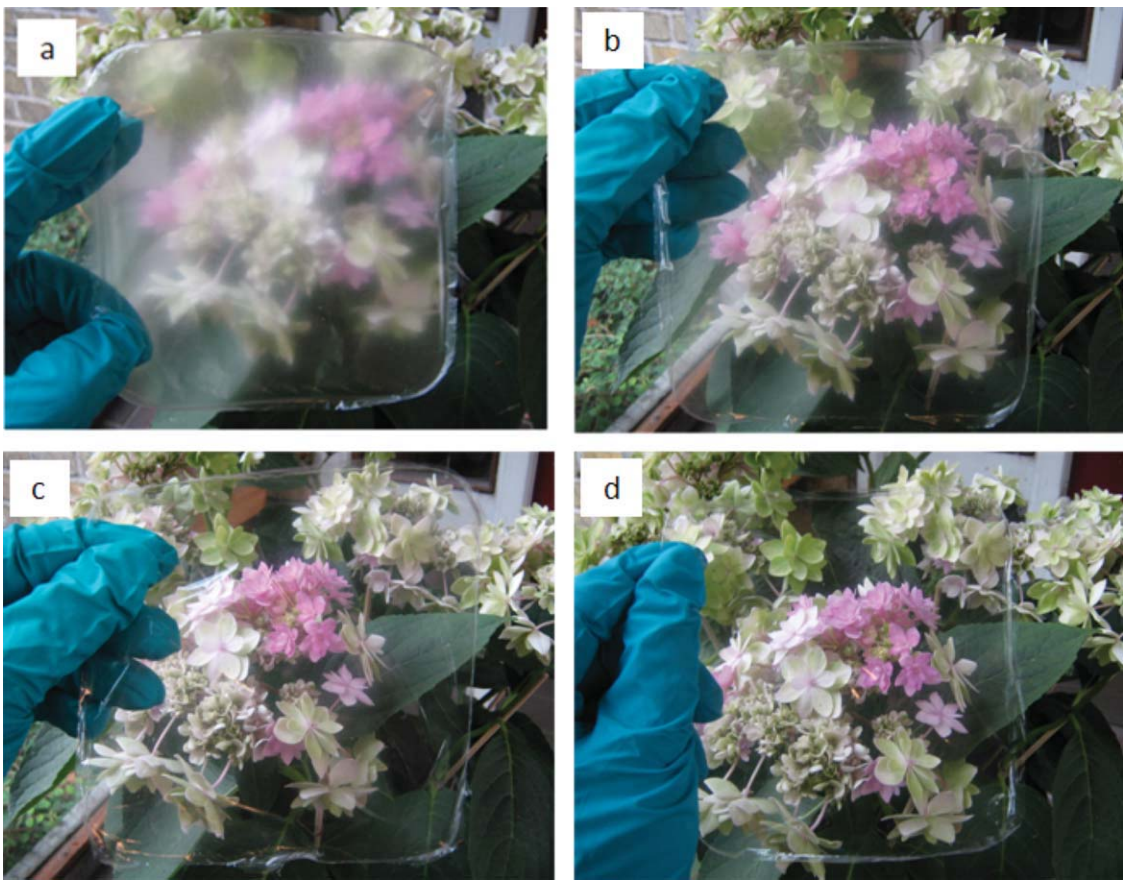

Figure 2 Visual transparency of the MFC 2 films: (a) 0p, (b) 1p, (c) 2p, and (d) 3p films. [Color figure can be viewed in the online issue, which is available at wileyonlinelibrary.com.]

Oxygen permeability (OP)

The oxygen transmission rate (OTR) of the MFC films was measured by means of a PBI-Dansensor OPT-5000 permeability tester (PBI-Dansensor, Ringsted, Denmark). Measurements were performed on 10-cm diameter films at 23°C and 50% RH with nitrogen as the carrier gas. The samples were conditioned for 3 days at 23°C and 50% RH before measurement. Poly(ethylene terephthalate) films were also tested as a reference. At least three samples of each film type were measured. The OTR was normalized with respect to the oxygen pressure gradient and film thickness to yield OP.

Statistical analyses

The significance of differences between samples obtained from the tensile and permeability test results was analyzed by student's two-tailed tests and by analysis of variance with the least-squares difference method of the general linear model procedure of SPSS 11.0 for Windows (Chicago, IL). Differences were considered significant at the $p > 0.05$ level.

RESULTS AND DISCUSSION

Visual properties

The appearance of the prepared MFC 2 films is shown in Figure 2. Films made from pulp 0p had limited transparency because of the presence of large fiber fragments and fiber aggregates, which could be seen with the naked eye. However, visual transparency was significantly improved by further homogenization steps. Only one additional homogenization step was required to produce a less opaque film [see the 1p film in Fig. 2(b)]. The 2p and 3p films, prepared from gels that were homogenized four and five times, respectively, had a high transparency [Fig. 2(c,d)].

Light transmittance of the MFC films and gels

The transparency of the various MFC 2 films was compared at 580 nm, with values normalized to a 25-μm film thickness. Light transmittance values of 60.9 ± 1.1, 68.0 ± 0.7, 75.0 ± 1.2, and 82.5 ± 0.5% were measured for the 0p, 1p, 2p, and 3 p films, respectively. Recently, Fukuzumi et al.[29] reported light transmittance as high as 90% through 20-μm films prepared from TEMPO-oxidized cellulose

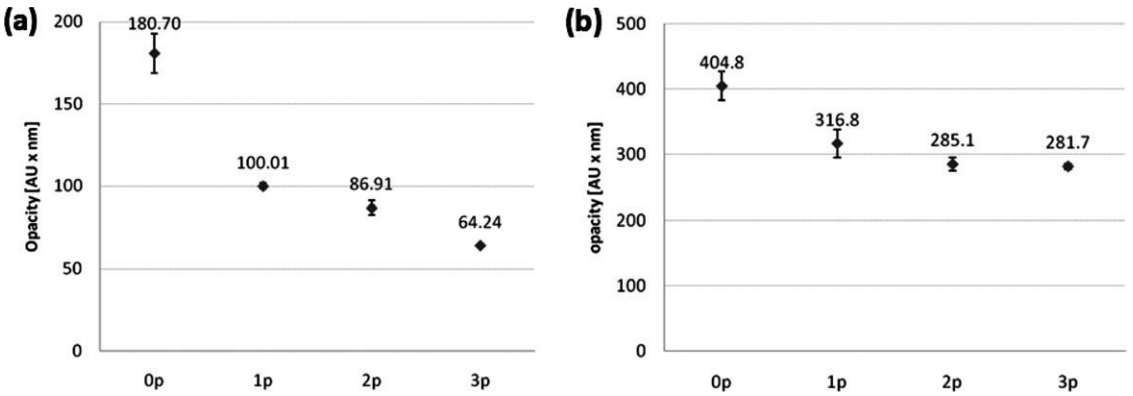

Figure 3 Opacity values of the (a) MFC 2 films and (b) diluted MFC 2 gels (0.35 wt %) as calculated from absorbances in the range 200–800 nm. The absorbance was normalized for 25-μm films. Data are expressed as the mean values of three replicates plus or minus the standard deviations.

nanofibers. However, in their study, unfibrillated and partly fibrillated fibers were removed from the gel by filtration through a nylon cloth with 20-μm pores. Aulin et al.[30] used carboxymethylated MFC from the same source as in this study to prepare MFC films and reported light transmittance values of 25 and 90% for 5.1 μm thick films homogenized 1 and 10 times, respectively. Figure 3 shows the opacity of the MFC 2 films [Fig. 3(a)] and gels [Fig. 3(b)] calculated from the visible spectra (not shown) according to the method of Gontard et al.[27] As shown, the disintegration of large fiber fragments via extra homogenization steps resulted in a reduction in the opacity in both the MFC 2 gels and films. The most significant difference was observed between samples 0p and 1p, whereas the decrease in opacity was not as pronounced for the other samples (1p–3p).

Optical microscopy

Figure 4 shows the optical microscopy images of the MFC 2 films. In our earlier research, no large fiber aggregation was observed in the case of MFC 1 films, which suggested adequate fibrillation.[26] The

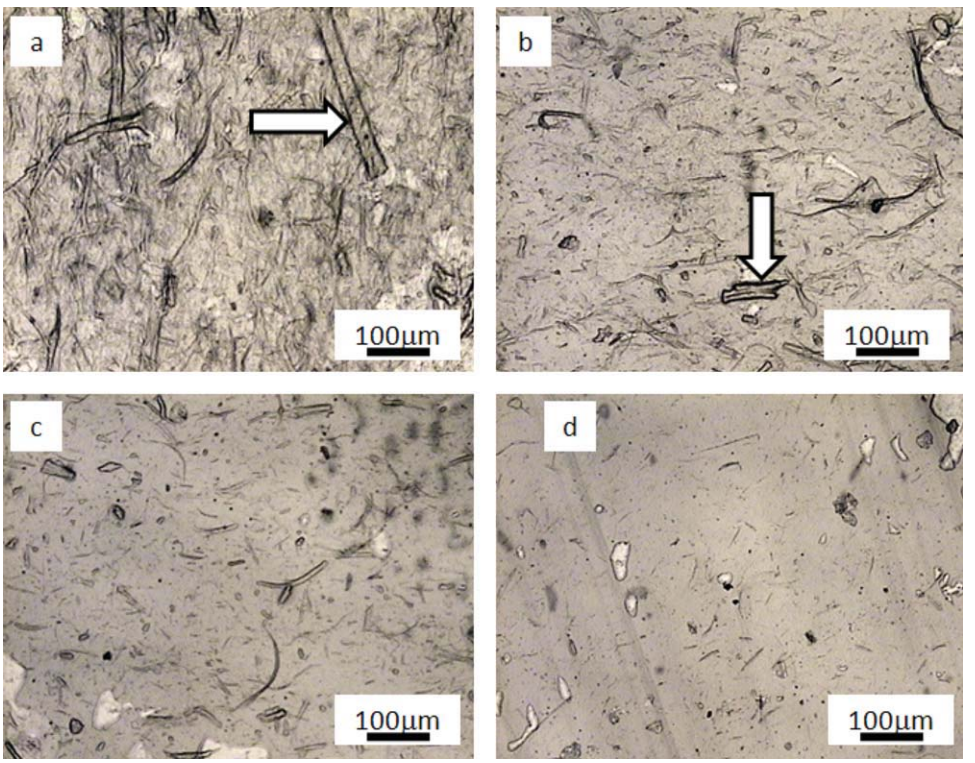

Figure 4 Optical microscopic images of the MFC films: (a) 0p, (b) 1p, (c) 2p, and (d) 3p films. The scale bars correspond to 100 μm. The arrows in parts a and b highlight the coarse fibers. [Color figure can be viewed in the online issue, which is available at wileyonlinelibrary.com.]

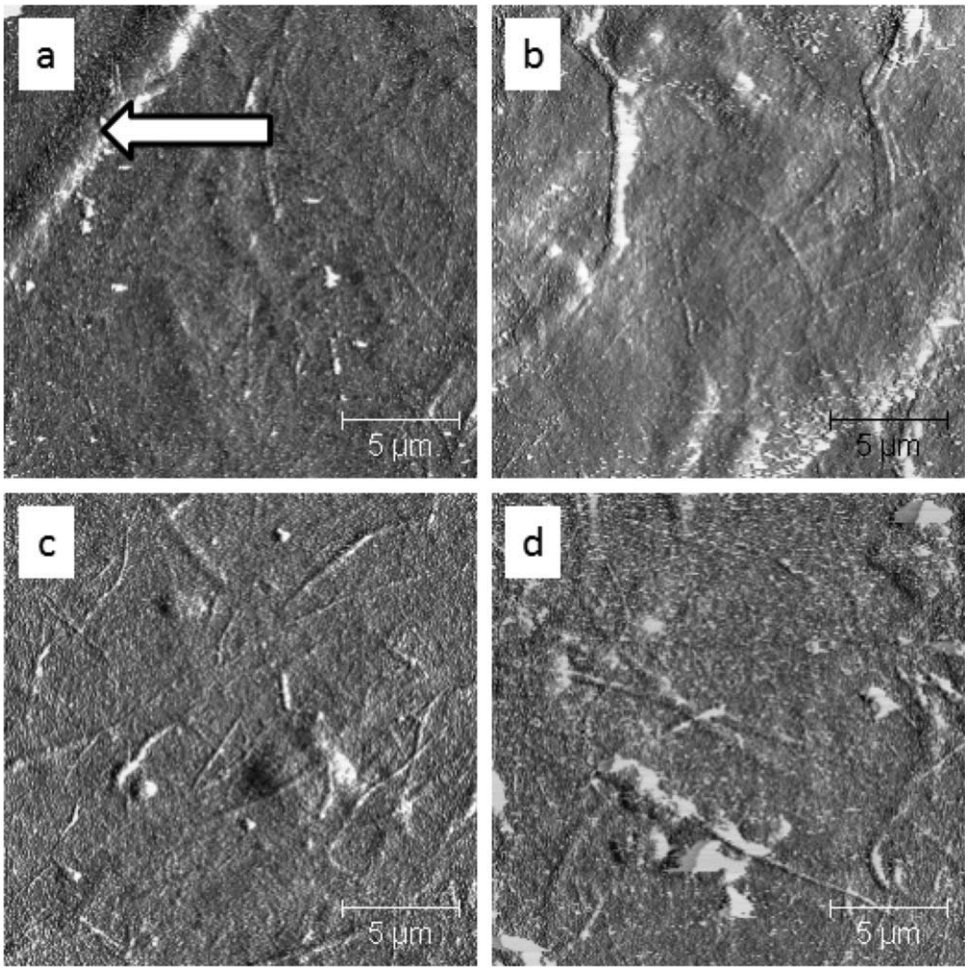

Figure 5 AFM phase images of the MFC 2 films: (a) 0p, (b) 1p, (c) 2p, and (d) 3p films. The scale bar corresponds to 5 μm. The arrow in part (a) highlights a micrometer-size fiber aggregate.

diameter size distribution of different fiber fragments and fiber aggregates in the MFC 2 films estimated by image processing was found to be very inhomogeneous. The diameter of the largest aggregates was about 25–30 μm, but smaller aggregates were also present with diameters of about 7–10 μm. As shown in the photomicrographs, the number of fiber fragments and fiber aggregates present in the films decreased with further homogenization steps. In addition to a decrease in the lateral dimensions by visual assessment the length of the fiber fragments also appeared to decrease with increasing homogenization [as indicated in Figs. 4(a,b)].

Atomic force microscopy

AFM was used to investigate the fiber structure in the micrometer- and submicrometer-size range on the film surfaces (Fig. 5). The presence of fiber aggregates was also apparent in the AFM images, in particular in that of the 0p films [Fig. 5(a)]. The size of these structures was generally in the 3–5-μm range; however, smaller fiber aggregates in the nanometer range were also observed. The AFM results confirmed that both the diameter and the length of the fiber aggregates on the film surfaces decreased with additional homogenization, as shown in Figure 5(b–d).

X-ray diffractometry

The degree of cellulose crystallinity is known to influence the mechanical and barrier properties of cellulose films, and therefore, it was important to determine the crystallinity in this case.[31,32] Figure 6 presents typical X-ray diffractograms of the MFC films prepared from the various gels. The main peak (I_{200}) appearing at $2\theta \approx 26^\circ$, was attributed to the crystalline parts of the MFC fibrils and was characteristic of cellulose I. The estimated relative crystallinity was about 60% for all film types; this indicated that there was no significant change in the crystallinity as a result of increasing homogenization. Similar crystallinity values (54.4–64.5%) were reported by Aulin et al.[33] for carboxymethylated MFC.

The influence of mechanical disintegration on the cellulose crystallinity has been investigated by other

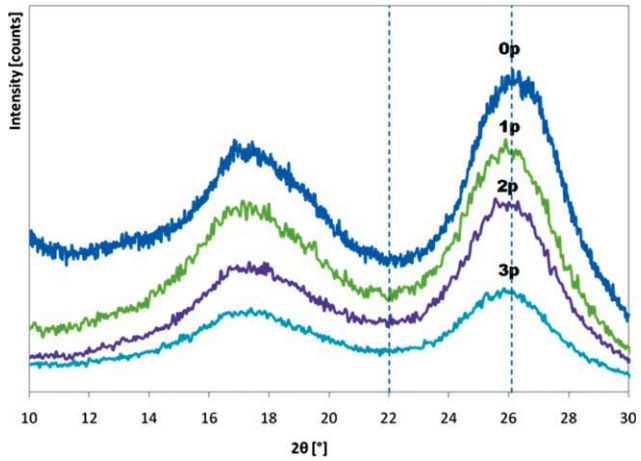

Figure 6 X-ray diffraction patterns of the MFC 2 films. [Color figure can be viewed in the online issue, which is available at wileyonlinelibrary.com.]

researchers[12,23] with contrasting results. For example, a crystallinity index of 49% was reported by Eyholzer et al.[12] for nanofibrillated cellulose prepared from carboxymethylated bleached beech pulp. These authors also indicated that the mechanical disintegration of the pulp significantly decreased its crystallinity (i.e., from 63 to 49%). On the other hand, mechanical treatment of a noncarboxymethylated pulp from the same source did not result in crystallinity reduction.[12] Iwamoto et al.[23] suggested that repeated passes through a homogenizer might cause a reduction in the cellulose crystallinity; however, no explanation for this phenomenon was presented.

Tensile tests

The mechanical properties of MFC films have been investigated by other researchers, and the values reported have generally been in the range 2.5–17.5 GPa, 80–312 MPa, and 2.1–11.5% for Young's modulus, strength, and strain at break, respectively. The relatively large scatter can be explained by the diversity of raw materials, fibrillation processes, and film preparation methods.[15] The tensile strength, modulus, and strain at break values measured here for the MFC 2 films are presented in Figure 7 and are within the range of overall values reported in the literature for MFC films. For example, in a study by Fukuzumi et al.,[29] TEMPO-oxidized softwood pulp was used to prepare MFC films, and the mechanical properties were similar to those measured here (233 ± 44 MPa, 6.9 ± 1.4 GPa, and 7.6 ± 0.2% for the strength, modulus, and strain at break, respectively). These authors applied a filtration process to remove unfibrillated and partly fibrillated fibers (>20 μm), and therefore, these tensile values might be compared to those for the 2p and 3p films (i.e., films free of large fiber aggregates). Henriksson et al.[34] investigated the tensile properties of MFC films made from carboxymethylated pulp. A modulus of 13.2 ± 0.6 GPa and a tensile strength of 214 ± 6.8 MPa were reported, whereas the strain at break was 10.1 ± 1.4% for such films.

The impact of additional homogenization steps on the mechanical properties of the MFC 2 films was also considered in this study. As indicated in Figure 7(a), no statistically significant difference ($p \leq 0.05$) in tensile strength was found between the MFC films as a function of the number of homogenization steps

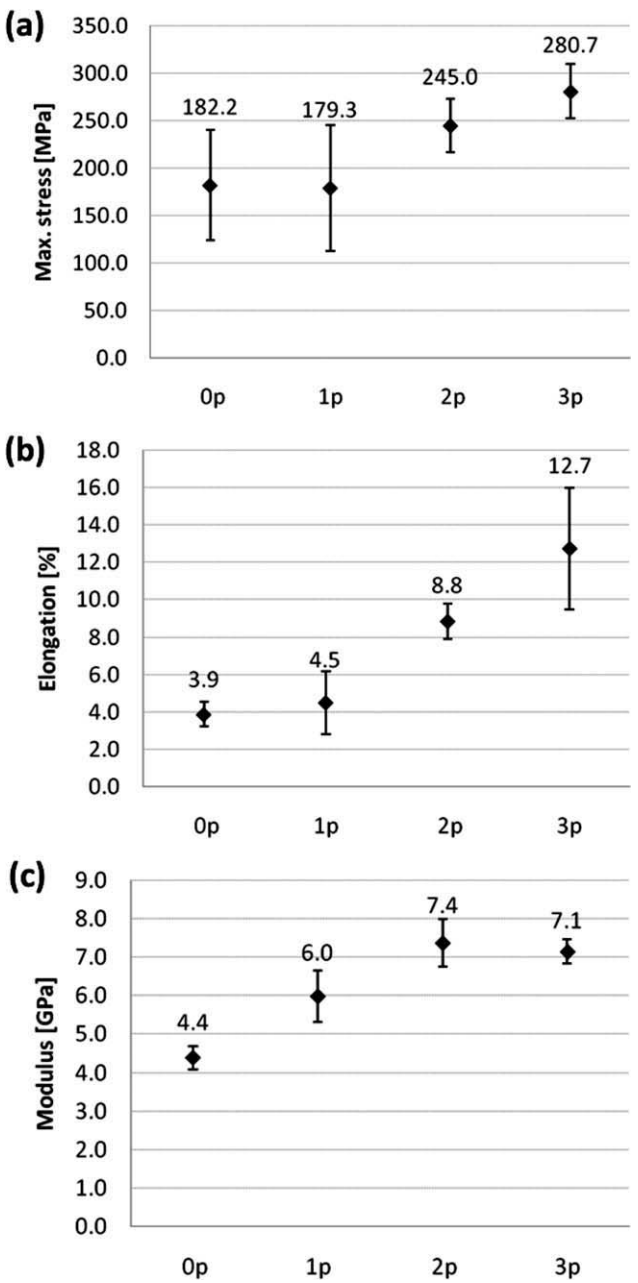

Figure 7 Tensile properties of the different MFC films: (a) maximal stress (MPa), (b) strain at break (%), and (c) Young's modulus (GPa). Data are expressed as the mean values of 10–15 replicates plus or minus standard deviations.

with the exception of films produced from gels passed through three additional homogenization steps (i.e., 3p film). These films had significantly higher strength than the 0p or 1p films. The extensibility of the film samples showed a tendency to increase with the number of homogenization steps, with the 2p and 3p films exhibiting significantly higher ($p > 0.05$) strain at break than the 0p and 1p films [Fig. 7(b)]. The highest strain observed was about 13%. An increase in Young's modulus is also shown in Figure 7(c) as a consequence of homogenization of MFC; however, the last homogenization step (i.e., production of the 3p gel) resulted in no further improvement in the average film modulus. A slightly lower average modulus was calculated for the 3p samples (7.1 GPa) than for the 2p samples (7.4 GPa), but this difference was not considered statistically significant.

The interpretation of these results was complicated by the complex structure–mechanical property relationships in nanofiber-based films; however, in the case of the MFC 2 films, we might argue that the finer nanofiber dimensions could have generated a more tightly packed structure with much smaller and more homogeneously distributed defects (i.e., voids), and for example, this could produce a film with superior strength when compared with MFC 1 films.[26] On the other hand, remnant fiber fragments and fiber aggregates may have acted as fracture-initiating points in the matrix built up by the entangled network of cellulose nanofibers. As illustrated here, these fiber fragments or fiber aggregates were disintegrated by additional homogenization, which may explain the superior mechanical properties for the 2p and 3p film samples. The importance of homogeneous fibrillation has also been demonstrated by other researchers. For example, Stelte and Sanadi[35] reported that the mechanical properties of cellulose fiber films prepared from softwood pulp improved with increasing homogenization until complete fibrillation was reached. This was credited to increased interaction between the nanofibers due to the higher degree of fibrillation. On the other hand, when fibrillated pulp was further homogenized, the modulus, strength, and strain started to decline. Other researchers have suggested that excess repeated passes through a homogenizer may result in the degradation of pulp fibers and a decrease in the fiber aspect ratio.[36] Indeed, as argued by Iwamoto et al.,[36] degraded, low-aspect-ratio fibers were rigid and easy to pull out from the aggregation of fibers, and therefore, MFC sheets made by short fibers were more brittle than those with a higher aspect ratio. These authors reported reduced mechanical properties (i.e., decreasing Young's modulus, strength, and strain) of MFC sheets with increasing number of passes through a grinder, which was attributed to decreases in the degree of polymerization and crystallinity. However, Zimmermann et al.[37] found that homogeneous fibrillation could be more important for the mechanical performance than the degree of polymerization of the cellulose. In our study, further homogenization steps were needed to obtain improved mechanical properties through complete fibrillation.

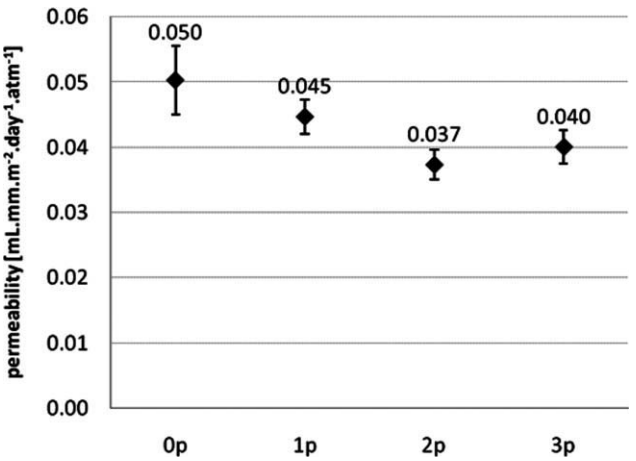

Figure 8 OP of different MFC films (0p–3p) measured at 23°C and 50% RH. Data are expressed as the mean values of three replicates plus or minus standard deviations.

Oxygen permeability

The effect of increasing homogenization on the OP of the MFC 2 films at 23°C and 50% RH is illustrated in Figure 8. Although decreasing mean OP values were observed, the differences were not statistically significant ($p > 0.05$). Other researchers also reported that the OTR of carboxymethylated MFC films is independent of the number of homogenization steps.[30] These authors reported an OP of 0.085 mL mm m^{-2} day^{-1} atm^{-1} for MFC films measured at 23°C and 50% RH. All the films in this study exhibited very low OP values in the range 0.04–0.05 mL mm m^{-2} day^{-1} atm^{-1}. These results were consistent with our earlier measurements of the MFC 2 film permeability[26] and provide OP values comparable with those found for good oxygen barriers, such as poly(vinylidene chloride) or poly(vinyl alcohol), measured under the same conditions.[38]

The high oxygen barrier properties characteristic of MFC films might have been due to the closely packed nanofibrillar structure, as illustrated by SEM (Fig. 9). The structure appeared paperlike, being lamellar and dense. Some cracks appeared parallel to the cellulose layers, which may have occurred during sample preparation. The degree of crystallinity may also have contributed to the high barrier properties because, as reported elsewhere,[31] the crystalline regions of cellulose are highly impermeable to oxygen molecules. Therefore, it is possible that the very dense nanofiber

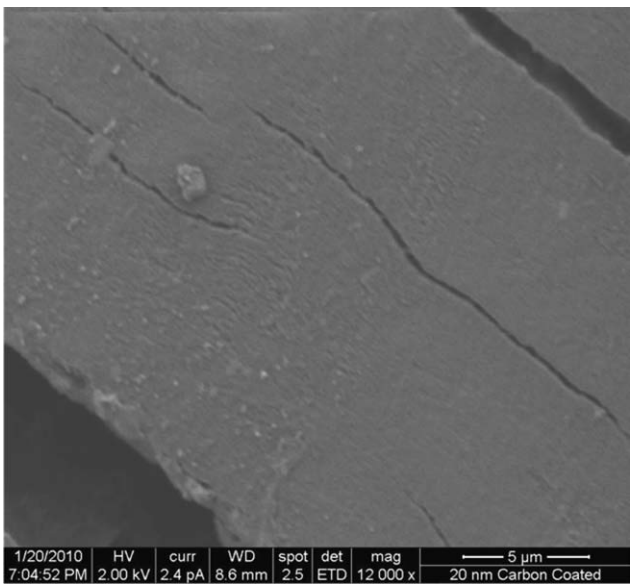

Figure 9 SEM image of the cross section of the MFC 2 film. The scale bar corresponds to 5 µm.

network combined with areas of high crystallinity explained the low OP data reported here and elsewhere.[29,30,39] The relative contribution of the cellulose crystallinity and film structure to the oxygen barrier properties in MFC films has yet to be resolved.

CONCLUSIONS

The research described in this article explored the effect of multiple processing steps on the properties of films cast from MFC gels. The raw material was a carboxymethylated sulfite-softwood-dissolving pulp with a low hemicellulose content. Larger fiber fragments and fiber aggregates in MFC films cast from gels processed once through a high-shear homogenizer compromised film transparency; however, these structures were eliminated, and film transparency was enhanced by a further two homogenization steps. This improvement in transparency was achieved without the sacrifice of mechanical properties. Indeed, the strain at break and modulus increased when a gel was used that had been homogenized four times; however, additional homogenization provided no further statistically significant changes in these properties. To summarize, we showed that carboxymethylated MFC gels could be converted to highly transparent oxygen-barrier films, albeit, at the cost of additional homogenization steps.

The authors thank David Nordqvist (Kungliga Tekniska Högskolan), Christian Bender Koch (Faculty of Life Sciences, Copenhagen University), and Vimal Katiyar (Risø Technical University of Denmark) for their help with aspects of the tensile testing, X-ray diffraction, and TEM. Guidance in the use of AFM from Noemi Rozlosnik (Technical University of Denmark Nanotech) was appreciated. The authors acknowledge Åsa Blademo at Innventia for the production of the MFC gels. The research of I. Siró was also supported by the Danish Research Council for Technology and Production Sciences.

References

1. Diddens, I.; Murphy, B.; Krisch, M.; Müller, M. Macromolecules 2008, 41, 9755.
2. Yano, H.; Nakahara, S. J Mater Sci 2004, 39, 1635.
3. Nogi, M.; Iwamoto, S.; Nakagaito, A. N.; Yano, H. Adv Mater 2009, 21, 1595.
4. Nogi, M.; Yano, H. Appl Phys Lett 2009, 94, 233117.
5. Herrick, F. W.; Casebier, R. L.; Hamilton, J. K.; Sandberg, K. R. J Appl Polym Sci Appl Polym Symp 1983, 37, 797.
6. Turbak, A. F.; Snyder, F. W.; Sandberg, K. R. J Polym Sci Polym Symp 1983, 37, 815.
7. Andresen, M.; Johansson, L. S.; Tanem, B. S.; Stenius, P. Cellulose 2006, 13, 665.
8. Abe, K.; Iwamoto, S.; Yano, H. Biomacromolecules 2007, 8, 3276.
9. Höpfner, S.; Ratke, L.; Milow, B. Cellulose 2008, 15, 121.
10. Pääkkö, M.; Vapaavuori, J.; Silvennoinen, R.; Kosonen, H.; Ankerfors, M.; Lindström, T.; Berglund, L. A.; Ikkala, O. Soft Matter 2008, 4, 2492.
11. Aaltonen, O.; Jauhiainen, O. Carbohydr Polym 2009, 75, 125.
12. Eyholzer, C.; Bordeanu, N.; Lopez-Suevos, F.; Rentsch, D.; Zimmermann, T.; Oksman, K. Cellulose 2010, 17, 19.
13. Eriksen, O.; Syverud, K.; Gregersen, O. Nord Pulp Pap Res J 2008, 23, 299.
14. Ankerfors, M.; Lindström, T. Presented at the 9th International Conference on Wood & Biofiber Plastic Composites, Madison, WI, May 2007.
15. Siró, I.; Plackett, D. Cellulose 2010, 17, 459.
16. Wågberg, L.; Decher, G.; Norgren, M.; Lindström, T.; Ankerfors, M.; Axnas, K. Langmuir 2008, 24, 784.
17. Lindström, T. Wochenblatt Für Papierfabrikation 1982, 110, 848.
18. Lindström, T.; Carlsson, G. Svensk Papperstid 1982, 85, R146.
19. Beghello, L.; Lindström, T. Nord Pulp Pap Res J 1998, 13, 269.
20. Hirota, M.; Tamura, N.; Saito, T.; Isogai, A. Cellulose 2009, 16, 841.
21. Saito, T.; Hirota, M.; Tamura, N.; Kimura, S.; Fukuzumi, H.; Heux, L.; Isogai, A. Biomacromol 2009, 10, 1992.
22. Saito, T.; Yanagisawa, M.; Isogai, A. Cellulose 2005, 12, 305.
23. Iwamoto, S.; Abe, K.; Yano, H. Biomacromol 2008, 9, 1022.
24. Bardage, S.; Donaldson, L.; Tokoh, C.; Daniel, G. Nord Pulp Pap Res J 2004, 19, 448.
25. Virtanen, T.; Maunu, S. L.; Tamminen, T.; Hortfing, B.; Liitia, T. Carbohydr Polym 2008, 73, 156.
26. Plackett, D.; Anturi, H.; Hedenqvist, M.; Ankerfors, M.; Gällstedt, M.; Lindström, T.; Siró, I. J Appl Polym Sci, 2010, 117, 3601.
27. Gontard, N.; Guilbert, S.; Cuq, J. L. J Food Sci 1992, 57, 190.
28. Segal, L.; Creely, J. J.; Martin, A. E. J.; Conrad, C. M. Text Res J 1959, 29, 786.
29. Fukuzumi, H.; Saito, T.; Wata, T.; Kumamoto, Y.; Isogai, A. Biomacromolecules 2009, 10, 162.
30. Aulin, C.; Gällstedt, M.; Lindström, T. Cellulose 2010, 17, 559.
31. Lagaron, J. M.; Catala, R.; Gavara, R. Mater Sci Tech 2004, 20, 1.
32. Eichhorn, S. J.; Young, R. J. Cellulose 2001, 8, 197.
33. Aulin, C.; Ahola, S.; Josefsson, P.; Nishino, T.; Hirose, Y.; Österberg, M.; Wågberg, L. Langmuir 2009, 25, 7675.
34. Henriksson, M.; Berglund, L. A.; Isaksson, P.; Lindström, T.; Nishino, T. Biomacromolecules 2008, 9, 1579.
35. Stelte, W.; Sanadi, A. R. Ind Eng Chem Res 2009, 48, 11211.
36. Iwamoto, S.; Nakagaito, A. N.; Yano, H. Appl Phys A 2007, 89, 461.
37. Zimmermann, T.; Bordeanu, N.; Strub, E. Carbohydr Polym 2010, 79, 1086.
38. Lange, J.; Wyser, Y. Pack Tech Sci 2003, 16, 149.
39. Syverud, K.; Stenius, P. Cellulose 2009, 16, 75.